Accepted Manuscript

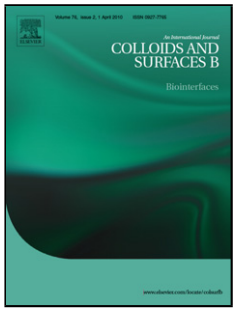

Title: Solid-state, triboelectrostatic and dissolution characteristics of spray-dried piroxicam-glucosamine solid dispersions

Author: Adeola O. Adebisi Waseem Kaialy Tariq Hussain Hiba Al-Hamidi Ali Nokhodchi Barbara R. Conway Kofi Asare-Addo

PII: S0927-7765(16)30534-3
DOI: http://dx.doi.org/doi:10.1016/j.colsurfb.2016.07.032
Reference: COLSUB 8037

To appear in: *Colloids and Surfaces B: Biointerfaces*

Received date: 23-3-2016
Revised date: 11-7-2016
Accepted date: 14-7-2016

Please cite this article as: Adeola O.Adebisi, Waseem Kaialy, Tariq Hussain, Hiba Al-Hamidi, Ali Nokhodchi, Barbara R.Conway, Kofi Asare-Addo, Solid-state, triboelectrostatic and dissolution characteristics of spray-dried piroxicam-glucosamine solid dispersions, Colloids and Surfaces B: Biointerfaces http://dx.doi.org/10.1016/j.colsurfb.2016.07.032

This is a PDF file of an unedited manuscript that has been accepted for publication. As a service to our customers we are providing this early version of the manuscript. The manuscript will undergo copyediting, typesetting, and review of the resulting proof before it is published in its final form. Please note that during the production process errors may be discovered which could affect the content, and all legal disclaimers that apply to the journal pertain.

ACCEPTED MANUSCRIPT

Solid-state, triboelectrostatic and dissolution characteristics of spray-dried piroxicam-glucosamine solid dispersions

Adeola O. Adebisi[a], Waseem Kaialy[b], Tariq Hussain[c], Hiba Al-Hamidi[d], Ali Nokhodchi[e,f], Barbara R. Conway[a], Kofi Asare-Addo[a]*

[a]Department of Pharmacy, University of Huddersfield, Huddersfield, HD1 3DH, UK

[b]School of Pharmacy, University of Wolverhampton, Faculty of Science and Engineering, Wolverhampton, WV1 1LY, UK

[c]The Wolfson Centre for Bulk Solids Handling Technology, Medway School of Engineering, University of Greenwich, Kent, UK

[d]Medway School of Pharmacy, Universities of Kent, Central Avenue, Kent, ME4 4TB, UK

[e]School of Life Sciences, University of Sussex, Arundel Building, Falmer, Brighton, BN1 9QJ, UK

[f]Drug Applied Research Center and Faculty of Pharmacy, Tabriz Medical Sciences University, Tabriz, Iran

*Corresponding author (Kofi Asare-Addo)

e-mail: k.asare-addo@hud.ac.uk

Tel: +44 1484 472360

Fax: +44 1484 472182

Submitted to: Colloids and Surfaces B

ACCEPTED MANUSCRIPT

Highlights

1. The spray drying process produced polymorphic transformations in **(piroxicam)** PXM

2. **Glucosamine (**GLU**)** improved dissolution in spray dried samples

3. GLU generally exhibited lower charge densities as compared to PXM

4. GLU improved the handling of PXM as it significantly reduced its charge in all the spray dried formulations.

5. Technique could be used to determine appropriate formulations that improve handling

Abstract

This work explores the use of both spray drying and D-glucosamine HCl (GLU) as a hydrophilic carrier to improve the dissolution rate of piroxicam (PXM) whilst investigating the electrostatic charges associated with the spray drying process. Spray dried PXM:GLU solid dispersions were **prepared** and characterised (XRPD, DSC, SEM). Dissolution and triboelectric charging was also conducted. **The** results showed **that the** spray dri**ed** PXM alone**,** without GLU produced some PXM form II **(DSC results)** with no enhancement in solubility relative to that of the parent PXM. **XRPD results also showed the spray drying process to decrease the crystallinity of GLU and solid dispersions produced.** The presence of GLU improved the dissolution rate of PXM. Spray dried PXM: GLU at a ratio of 2:1 had the most improved dissolution. **The spray drying process generally yielded PXM-GLU spherical particles of around 2.5 µm which may have contributed to the improved dissolution.** PXM showed a higher tendency for charging in comparison to the carrier GLU (- 3.8 *versus* 0.5 nC/g for untreated material and -7.5 *versus* 3.1 nC/g for spray dried materials). Spray dried PXM and spray dried GLU demonstrated higher charge densities than untreated PXM and untreated GLU, respectively. Regardless of PXM:GLU ratio, all spray dried PXM:GLU solid dispersions showed a negligible charge density (net-CMR: 0.1 – 0.3

ACCEPTED MANUSCRIPT

nC/g). Spray drying of PXM:GLU solid dispersions can be used to produce formulation powders with practically no charge and thereby improving handling as well as dissolution behaviour of PXM.

Keywords: Solid dispersions; Piroxicam; D-glucosamine HCl; Dissolution; Electrostatics; Spray drying.

Abbreviations: GLU, D-glucosamine hydrochloride; DSC, differential scanning calorimetry; XRPD, X-ray powder diffraction; FTIR, Fourier transform infra-red; BCS, biopharmaceutical classification system; CBZ, carbamazepine; PXM, piroxicam; NSAID, non-steroidal anti-inflammatory drug; DE, dissolution efficiency; MDT, mean dissolution time; MDR, mean dissolution rate; ATR, attenuated total reflection; PSD, particle size distribution; USP, United States pharmacopoeia; PM, physical mixture.

1. Introduction

The physiochemical properties of a drug can influence the choice of dosage form in which it is delivered. Properties such as stability, pK_a, partition coefficient and salt forms are all taken into consideration during pre-formulation studies [1]. In addition, it is important to assess the aqueous solubility, dissolution rate and intestinal permeability of a drug. These three factors have been used to classify drugs in the Biopharmaceutical Classification System (BCS) into four different classes [2]. BCS class II drugs are characterized by high membrane permeability but low aqueous solubility therefore; there is a low drug concentration gradient between the gut and the blood vessels limiting drug transport and oral bioavailability. The poor solubility of drugs has always been a major problem in pharmaceutical development and this problem is now more prevalent with more than 40 % of the new chemical entities being practically insoluble in water or lipophilic in nature [3-7]. As dissolution rates are typically the rate-limiting step for bioavailability, especially for poorly soluble drugs, enhancement of solubility is vital to attaining suitable systemic concentrations for therapeutic effect [8].

ACCEPTED MANUSCRIPT

Despite the recent advances in particle engineering, one of the most common method employed to aid the improvement of the dissolution rate of poorly soluble drugs is particle size reduction using high shear milling methods [9, 10]. This enhancement of dissolution rate by size reduction is due to the fact that solubility of drugs in intrinsically related to particle size of the drug [7]. As the particle size of the drug is reduced, the surface area available for solvation also increases. Particle size reduction is a safe method of increasing drug dissolution without altering the chemical nature of the drug. However, although particle size reduction leads to an increase in the effective surface area of the drug available to interact with the solvent, it does not increase equilibrium solubility of the drug [11] unless the size of particles are reduced to below 1 micrometre [12]. In addition, micronization may cause agglomeration and thus may negatively impact on the solubility and bioavailability during the storage of the final product [13]. Moreover, milled particles usually exhibit **a** high level of electrostatic charge; such high level of charge can increase the inter-particle cohesive forces leading to poor product performance [14-16].

Other methods used to improve drug solubility include complexation [17], liquisolid techniques [18, 19] and salt formation [20, 21]. Several authors have classed the solid dispersion approach as one of the most effective method of improving dissolution of drugs [5, 8, 22]. It involves the dispersion of one or more active ingredients in an inert excipient or carrier, where the active ingredients could exist in a finely crystalline, solubilised or amorphous state [23, 24]. Solid dispersion also enhances the absorption and efficacy of drugs in a dosage form, despite limitations such as cost, scale up and physicochemical instabilities of the dispersions under normal storage conditions [25-27]. Al-Hamidi and co-workers have studied the rate of carbamazepine (CBZ), ibuprofen (IBU) and PXM (PXM) in solvent evaporated and co-ground solid dispersions [3, 22, 28, 29]. Asare-Addo *et al* [8], also studied the effect of GLU on indomethacin (IND) dissolution and charging properties using a solvent evaporation process. All these authors showed that incorporation of GLU in PXM, IBU, CBZ and IND using either the solvent evaporation or grinding method significantly increased the dissolution rates of these drugs. They attributed the increased

ACCEPTED MANUSCRIPT

solubility and dissolution rate of drugs observed to be due to particle size reduction to sub-micron levels, change in polymorphic forms and the improved wettability of the drug particle by the dissolved hydrophilic carrier [28, 30].

PXM (4-hydroxy-2-methyl-N-(2-piridyl) 2H-1,2-benzothiazine-3-carboxamide-1, 1-dioxide) is one of the most potent non-steroidal anti-inflammatory and analgesic drugs used in treatment of various acute and chronic musculoskeletal and joint disorders [31]. This drug was used as the model BCS class II drug. In addition, GLU was the preferred hydrophilic carrier due to its popular use as a nutritional supplement for humans in decreasing pain and improving mobility in osteoarthritic joints of humans when administered orally [32, 33]. The limited solubility of PXM leads to a delayed onset of therapeutic effect. Oral absorption is slow and gradual with maximum absorption occurring 3 – 5 hours after administration and a long half-life of elimination [34].

Spray drying of poorly soluble drugs could potentially enhance their solubility [35]. The state of the final spray dried product depends on the nature of the drug as the process may result in the amorphous, partially crystalline, metastable crystal forms [36]. The ability of a pure drug substance to convert into its amorphous form during spray drying depends mainly on its inherent glass forming ability and crystallization tendency [37] and to a lesser extent on the preparation methods [38, 39]. In the amorphous state, the drug exhibits high levels of super-saturation in aqueous media compared to the crystalline drug, thereby achieving higher apparent solubility [40]. Spray drying works by providing a large surface area where heat transfer and atomization of the solution or suspension into small droplets can occur. It is also good at producing a uniform product that is spherical in shape [41]. By spraying the substance into a steam of hot air, the droplet will dry to form individual solid particles at a fast drying rate within milliseconds to a few seconds as a result of the high surface to volume ratio, which prevents phase separation between the drug and polymer components [42].

In pharmaceutical development field, characterization of the electrostatic properties of powders has become a subject of extensive research [43]. Electrostatic charging within powders is generated

ACCEPTED MANUSCRIPT

from inter-particulate contacts and collisions (particle-particle and particle-surface collisions) in a gaseous environment; i.e. two different materials brought to contact and then separated [44]. To date, there are no pharmacopoeial methods for charge characterization [45]. Although bipolar charging commonly takes place in industrial processes of pharmaceutical particulates [46], the most prevalent assessment of tribocharging is gained from the Faraday pail method, which provides only limited information in the form of net charge-to-mass ratio [47]. In this work, a novel instrument recently developed in the Wolfson Centre [48] (Figure 1a) to characterise the charge properties of the particulate materials under investigation in the form of charge distribution is used. The major advantages of this method of charge sensing include its high sensitivity (charges on the particles equal or more than to 30×10^{-15} C are detectable), quick measurement (< 1 min) and the lack of the particle flow disturbance. Kaialy *et al.* [16] applied the latter method to characterize the charge distribution of several size fractions of spray dried mannitol. In this study, the efficiency of the spray drying process in enhancing the dissolution rate of the PXM using GLU as a hydrophilic carrier is investigated. Recently, Adebisi *et al* (2016) [49], also utilized this methodology in determining the charge distribution in co-ground solid dispersions. The charging propensity of the solid dispersions produced as a result of the spray drying process is also assessed to determine its effect on the handling of these dispersions. To the best of our knowledge, there is no reported work that has investigated the use of GLU in spray dried solid dispersions and the charge distributions from resulting samples.

2. Materials and Methods

2.1. Materials

PXM was purchased from TCI Chemicals (Japan). GLU was purchased from Sigma-Aldrich (UK). The solvent used (acetone) was obtained from Fischer Scientific (UK) was of analytical grade and was used as obtained. The dissolution medium (pH 1.2) was prepared according to the USP 2003 method using the following materials: KCl (Sigma, UK) and concentrated HCl (Fisher, UK).

ACCEPTED MANUSCRIPT

2.2. Preparation of PXM-GLU physical mixtures

Physical mixtures (PM) of PXM were prepared by mixing PXM and GLU in a Turbula® blender (Type T2 C, Switzerland) for 10 min. Different PXM:GLU ratios (2:1, 1:1 and 1:2) were prepared for comparison. The powders were stored in screw-capped glass vials in a desiccator at room temperature until required after the mixing process.

2.3. Preparation of spray dried solid dispersions of drug-carrier

The spray drier (SD-06AG laboratory spray dryer, LabPlant UK) was set up in a closed mode configuration with an inlet temperature of 70 °C, a feed flow rate set to 10 mL min^{-1} and a nozzle size of 0.5 mm. Suspensions of PXM and GLU were made at three different drug:carrier ratios: 1:1 (Sample A) 1:2 (Sample B) and 2:1 (Sample C). When making the 1:1 ratio, 1.5 g of PXM was dissolved in a beaker containing 600 mL of acetone whereas 1.5 g of GLU was dissolved in a beaker containing 600 mL of deionised water under stirring conditions. The two solutions were then mixed together to form sample A. In the case of the 1:2 ratios, 1.5 g of PXM was dissolved in a beaker containing 600 mL of acetone and 3 g of GLU was also dissolved in a beaker containing 600 mL of deionised water. The two solutions were mixed together and that constituted sample B. For the 2:1 ratio, 3 g of PXM was dissolved in a beaker containing 600 mL of acetone and 1.5 g of GLU was also dissolved in a beaker containing 600 mL of deionised water. The two solutions were mixed together to form sample C. PXM (1.5 g PXM dissolved in 600 mL acetone) and GLU (1.5 g GLU dissolved in 600 mL deionised water) were also spray-dried separately as control samples. The suspensions were under constant stirring (200 rpm) throughout the feeding process into the spray dryer to ensure uniformity. The solid dispersions obtained were stored in a desiccator until required.

ACCEPTED MANUSCRIPT

2.4. Particle Size Analysis (PSD)

A Sympatec laser diffraction particle size analyser (Clausthal-Zellerfeld, Germany) was used for the determination of the particle size distribution of the spray-dried formulations. **The mean particle size ($D_{10\%}$, $D_{50\%}$ and $D_{90\%}$) was calculated automatically using the software provided.** The procedure was as follows: about 2–3 g of each sample was transferred into the funnel of the VIBRI (vibrator feeder). The sample container was cautiously tapped against the funnel to ensure all the content was transferred. A test reference measurement was performed with the HELOS sensor using WINDOX software followed by a standard measurement. **In this technique a laser beam is passed through the sample, and different size particles diffract the light at different angles to produce a particle size distribution [3]**.

2.5. Scanning electron microscopy (SEM)

Electron micrographs **of PXM, spray dried PXM, GLU, spray dried GLU and all the spray dried solid dispersion in the various ratios** were obtained using a scanning electron microscope (Jeol JSM-6060CV SEM) operating at 10 kV. The samples were mounted on a metal stub with double-sided adhesive tape and were sputter-coated with using a Quorum SC7620 Sputter Coater under vacuum with gold in an argon atmosphere prior to observation. Micrographs with different magnifications **of 500x, 100x, 3000x and 5000x** were taken to facilitate the study of the morphology of the solid dispersions.

2.6. Differential scanning calorimetry (DSC)

Samples of spray-dried solid dispersions or PM of drug:carrier (3 - 6 mg) were placed in standard aluminium pans (40 µL) with a vented lid. The crimped aluminium pans were heated from 20 to

ACCEPTED MANUSCRIPT

250 °C at a scanning rate of 10 °C/min using nitrogen gas as a purge gas in a DSC 1 (Mettler-Toledo, Switzerland). The enthalpy, onset temperatures and melting points of the samples were obtained using the STAR^{e} thermal analysis software.

2.7. X-ray powder diffraction (XRPD)

The untreated PXM, GLU and PXM-GLU solid dispersions were characterised by X-ray powder diffraction (XRPD) according to the methodology reported by Laity *et al* 2015 [50] using a D2 Phaser diffractometer (Bruker AXS GmbH, Karlsruhe, Germany), with a sealed microfocus generator operated at 30 kV and 10 mA, producing Cu_{Ka} (λ_X = 0.1542 nm) radiation and a Lynxeye 'silicon strip' multi-angle detector. The samples were scanned in Bragg-Brantano geometry, over a scattering (Bragg, 2θ) angle range from 5 to 100°, in 0.02° steps at 1.5° min^{-1}.

The XRPD patterns of were obtained using a Bruker D2 Phaser XRPD diffractometer. The samples were scanned from 5° to 10° 2 θ at a rate of 1.5° min^{-1}.

2.8. Solubility studies

Excess amount of the powder formulations were added to glass vials containing 10 mL of buffer (pH 1.2). The vials were sealed and placed into a Wise Bath WSB-18, where they were agitated at 37 °C ± 0.5 °C for 48 h. The solutions were then filtered using a 0.45 µm membrane filter (Whatman, UK) and the filtrates were diluted with buffer (pH 1.2) before the absorbance of these solutions were measured using a UV spectrophotometer (UV-160, Shimadzu, Nakagyo, Japan) at 333 nm. The drug concentration in the samples was determined by applying a calibration curve which had a correlation coefficient of **1**. The effects of GLU on the solubility of PXM were also

ACCEPTED MANUSCRIPT

investigated and this was achieved by the addition of an excess of PXM to 10 mL buffer (pH 1.2) containing GLU at 1, 5, 10 and 15 % w/v.

2.9. Dissolution studies

USP dissolution apparatus I (DT700, ERWEKA, Heusenstamm, Germany) was used to monitor the dissolution profiles of PXM, PXM-GLU PMs and spray-dried solid dispersions. All formulations for the dissolution process contained the same amount of PXM (20 mg of PXM content was used regardless of the carrier quantity). The powder samples, after weighing, were introduced into the dissolution basket. Circular paper discs were used to cover the base of the baskets. This was to prevent the drug powder falling through the bottom pores. The dissolution medium was at pH 1.2 (900 mL) equilibrated to 37 °C ± 0.5 °C with the baskets rotated at 50 rpm. Samples were withdrawn at selected time intervals (5, 10, 15, 20, 25, 30, 40, 50, 60, 75, 90, 105 and 120 min) using a peristaltic pump. The concentrations of PXM in the samples were determined by UV spectrophotometer at 333 nm. All dissolution tests were carried out in triplicate.

2.10. Dissolution parameters

As an independent metric, the mean percentage of drug dissolved in the first 10 min (Q_{10min}) and 30 min (Q_{30min}) were used to represent the dissolution rate from various preparations. The dissolution efficiency (DE) of a pharmaceutical dosage form is defined as the area under the dissolution curve up to the time, *t*, expressed as the percentage of the area of the rectangle [51] as detailed elsewhere [52, 53].

ACCEPTED MANUSCRIPT

$$\text{DE}\ (\%) = \frac{\int_0^t y \times dt}{y_{100} \times t} \times 100\%$$

where y is the percentage of drug dissolved at time t.

Another approach to obtain a parameter that describes the dissolution rate is the mean dissolution time (MDT). This parameter is the most likely time taken for a molecule to be dissolved from a solid dosage form. In other words, MDT is the mean time for the drug to dissolve under *in vitro* dissolution conditions and is calculated using the following equation:

$$\text{MDT (min)} = \frac{\sum_{j=1}^{n} t_j \Delta M_j}{\sum_{j=1}^{n} \Delta M_j}$$

where j is the sample number, t_j is the midpoint of the jth time period (calculated with ((t + t-1)/2) and ΔM_j is the additional amount of drug dissolved between t_j and t-1.

The mean dissolution rate (MDR) can be calculated according to the following equations:

$$\text{MDR } (\%\text{min}^{-1}) = \frac{\sum_{j=1}^{n} \Delta M_j / \Delta t}{n}$$

where n is the number of dissolution sample times, Δt is the time at the midpoint between t and t-1 (easily calculated with [t + (t-1)/2].

2.11. Similarity factor

ACCEPTED MANUSCRIPT

Similarity between the drug release profiles was determined using similarity factor f_2 according to the equation below [54-57]

$$f2 = 50\ log\left\{\left[1 + \frac{1}{n}\sum_{t=1}^{n} w_t(R_t - T_t)^2\right]^{-0.5} X\ 100\right\}$$

where *n* is the number of pull points for tested samples; w_t is the optional weight factor; R_t is the reference assay at time point *t*; T_t is the test assay at time point *t*.

Similarity factor was calculated using the drug release profile of the untreated piroxicam as the reference. f_2 values ranging from 50-100 indicate similarity between the two profiles. The closer the *f2* value is to 100, the more similar or identical the release profiles. Values of *f2* less than 50 indicate dissimilarity between two dissolution profiles [58, 59].

2.12. Triboelectric assessment of spray dried solid dispersions

The charge properties of powders were analysed using a recent novel approach developed at the in the Wolfson Centre at the University of Greenwich. In brief, a triboelectric device electrostatic inductive sensor was used to investigate the triboelectrification of powders under investigation [48]. Such novel method allows the detection and measurement of charge distribution on the charge sign basis in a population of particles. The experimental apparatus consists of a single non-contact electrostatic inductive sensor (probe), a charge amplifier unit, a national instrument (NI) data acquisition equipment and personal computer for data recording and processing. A sample of each powder was fed in the cylindrical sensor with the help of vibratory feeder and conveyed toward the sensor by gravity in a vertical direction. Special care was taken by considering the adhesion property of particles with the wall of the sensor. After each experiment, the inner tube was replaced in order to remove any deposits, impurities or surface charge that may have been present on the

ACCEPTED MANUSCRIPT

surface from a previous test. A fresh sample was used for each test experiment. Each sample was analysed six times (humidity and temperature controlled laboratory: 50% RH, 22 ºC). A typical example of processed charge signal obtained as a result of the untreated PXM particles moving through the sensor using vibratory orifice feeder under gravity is shown in Figure 1b. The direction of each peak shows the polarity of charged particles and amplitude from baseline and represents the amount of charge on moving particle. The positive charge is the sum of positive charges whereas the negative charge is the sum of negative charges. The net charge is the sum of positive charges and negative charges. The charge–to–mass ratio (CMR or charge density) was defined as the charge (negative charge for N–CMR, positive charge for P–CMR, net charge for net–CMR) per unit mass, in nC/g.

3. RESULTS AND DISCUSSION

Untreated PXM showed a DE of only 21.2 % over the 120 min interval (Table 1) demonstrating the reported poor solubility of PXM, which in turn affects its bioavailability. PXM is a drug administered via the oral route and it will have to pass through the first pass metabolic pathway, which further lowers its bioavailability. In order to achieve the desired therapeutic effect a high dose of the drug will have to be administered [22]. The poor dissolution characteristics of PXM may be due to poor wettability, where the dissolution media is unable to spread efficiently over the solid surfaces to bring about dissolution [29]. In addition, agglomeration of the drug particles could also limit solubility. The results from the spray-dried PXM and PMs indicated no significant difference in PXM dissolution regardless of PXM:GLU ratio (Figure 2a, Table 1) . **In order words, t**he dissolution of the spray-dried PXM and the PM over the 120 min interval was similar to that of the untreated PXM **(*f2* = 74-93)**. However, when the untreated PXM was mixed with spray-dried GLU in the ratios 1:1, 1:2 and 2:1 (Figure 2b), the results of the 1:1 and 1:2 PMs showed DE to increase from 21.2 % as observed in untreated PXM to 33.2 % and 38.0 %, respectively. ***f2* values**

ACCEPTED MANUSCRIPT

using the untreated PXM as the reference showed dissimilarity to occur for the 1:1 and 1:2 ratios (*f*2 = 46 and 39 respectively) thereby confirming the DE observations. These results showed that, in contrast to commercial GLU, mixing spray-dried GLU with PXM could enhance the dissolution of PXM. This may potentially be as a result of the change in morphology in the SEM images (Figure 3 and supplementary materials figure 1) of the spray dried GLU (smaller and less crystalline) and how the PXM may have attached on to them. This however was not true for the 2:1 PXM and spray-dried GLU **(*f*2 = 70)**. This sample had a DE value lower (DE_{120min} of 16.4 %) than that of the untreated PXM (DE_{120min} of 21 %) (Table 1). This may be due to the increased content of PXM in the formulation.

Generally, fine particulates tend to charge negatively, whereas large particles tend to charge positively. Lacks and Levandovsky, 2007 [60] provided a hypothetical mechanism for particle size dependent charging. Assuming that the surface density of trapped electrons is initially the same on all particles, it has been argued that the collisions allow electrons trapped in high-energy states on one particle to transfer to the vacant low-energy states on another particle. This has been recently discussed in a review [61]. Triboelectric charge analyses showed that all materials investigated demonstrated bipolar charge behaviour, i.e., contained both electropositive and electronegative charge particles. Untreated **PXM** showed an overall electronegative charge density (net-CMR = -3.8 ± 0.9 nC/g) (Figure 4a). Such charging may result in several problems attributed to particle agglomeration, segregation and/or material adhesion on the processing equipment. In contrast, untreated GLU showed a very slight tendency towards electropositive charge (net-CMR = 0.5 ± 0.4 nC/g) (Figure 4b). As seen in Figures 4a and b, PXM demonstrated a considerably higher absolute charge than GLU carrier. This may be due to differences in the inherent charging properties between PXM and GLU as well as the small size of PXM in comparison to GLU (Supplementary materials table 1) as it is known that electrostatic forces increase when particle size is decreased [16]. Both the electronegative charge density of PXM and the electropositive charge density of

ACCEPTED MANUSCRIPT

GLU increased following spray drying (~ 2.0 fold-increase in the case of PXM drug ~ 5.9 fold-increase in the case of GLU carrier) (Figures 4a, b). Triboelectric charge analyses showed spray dried PXM:GLU solid dispersions to have considerably lower charge density (-0.1 ± 0.1 – 0.3 ± 0.4 nC/g, $p > 0.05$) than untreated PXM (- 3.8 ± 0.9 nC/g) and untreated GLU (0.5 ± 0.4 nC/g) (Figure 5a). This shows the spray drying method applied reduced the charge of pure **PXM** and thus improves powder handling.

Figure 5b shows the dissolution of spray-dried PXM and GLU (samples A - C) and the results show an enhancement in dissolution as compared to the untreated PXM. The increase in dissolution of the spray dried solid dispersion samples is likely due to the formation of small particle sizes, increased surface area and potentially reduced inter-particle cohesive forces as indicated by a net charge density of less than 0.4 nC/g (Figure 5a). SEM images (Figure 3 and supplementary materials table 1) showed the appearance of the spray-dried samples to be very different from that of the parent drug and carrier. The spray drying process yielded spherical particles of around 2.5 µm but showed some agglomeration in Sample A, B and C with sample B showing some of the needle-like characteristics of PXM form II [62]. The needle form of PXM may have contributed to the poor dissolution of sample B as it has been reported that the form II PXM polymorph is less soluble than the Form I polymorph [63]. However, this was in contrast to the observations by other researchers who report an increase in solubility with the Form II polymorph [64, 65]. **This contrasting difference may be due to differences in in the preparation method as well as the contribution of the polymorphic form to the solubility. Lai et al. [65] reasoned that the cavitation forces as well as the collision and shear forces during the homogenising they conducted determines the breakdown of drug particles to the nanometre range. They deduced further that these high energetic forces can also induce a change in the crystal structure and/or partial or total amorphisation of the sample, which could cause further enhancement in solubility[66].**

ACCEPTED MANUSCRIPT

The dissolution results suggest that when PXM and GLU were spray-dried together, the 2:1 ratio (sample C) was the best in achieving the optimum level of dissolution enhancement. Sample C increased the dissolution of PXM by over 30 % in comparison to untreated PXM. Samples A - C (DE_{120min} of 31- 57 %) all had improved dissolution efficiency over that of the untreated PXM (DE_{120min} of 21 %).

With regards to solubility, Table 2 shows untreated PXM to have a solubility of 20.7 mg/L. Spray-dried PXM had a solubility of 17.7 mg/L which explained why the spray drying process did not improve dissolution. When the solubility tests were conducted with PXM in the presence of GLU at different concentrations, the solution containing 1 % w/v GLU had a solubility of 17.4 mg/L. This was also lower than the untreated PXM, which had a solubility of 20.7 mg/L. The solution containing 5 % w/v GLU also had solubility (20.1 %) slightly lower than that of the untreated PXM, however, this was an improvement from the 1 % w/v GLU. The solutions containing 10 % w/v and 15 % w/v GLU both experienced solubility enhancement in comparison to that of the untreated PXM (20.7 %) with solubilities of 22.8 and 23.4 % respectively. The results therefore suggested that solubility could be improved by increasing the proportion of GLU in the solutions. However, the same conclusion could not be made regarding the results from the dissolution test as there was no correlation (Table 1). Al-Hamidi *et al* 2010 [3] concluded that an improvement in dissolution rate cannot be correlated to solubility and that parameters such as particle size, type of polymorph and hydrophobicity of particle surfaces are responsible for enhancement in dissolution.

Untreated PXM had a melting point of 201.53 ˚C signifying the form I PXM polymorph (Supplementary materials figure 2) [67]. However after spray drying, the DSC scan of spray-dried PXM exhibited two peaks; one at 196.47 ˚C and the other at 199.72˚C. This may be due to the fact that the spray drying process led to the re-crystallization of some PXM molecules in the Form II (lower melting point) polymorph of PXM [63]. This observation can be confirmed in the SEM image of spray-dried PXM (Supplementary materials figure 1) as needle-shaped PXM particles that

ACCEPTED MANUSCRIPT

are characteristic of Form II PXM were also observed [68]. GLU appears as a single endothermic peak on the DSC trace (Supplementary materials figure 2) with a melting point at 210.27 ˚C. After spray drying however, it seems the characteristics of GLU were altered with the spray-dried GLU showing two distinct endothermic peaks on the DSC scans different from the peak observed from the untreated GLU. After further investigation, it was noticed that the untreated GLU DSC trace had a shoulder at the position of 222 - 225 ˚C. This was around the same position where the new peak appeared in spray-dried GLU and this suggests that the GLU also underwent some physical changes after spray drying. The DSC traces of the PM showed the PXM and GLU peaks to overlap (Supplementary materials figure 3). The melting points of the two materials are similar making the resultant peak of the PM to merge. It was observed that the intensity of the peaks varied as the ratio of each material varied in proportion. The DSC traces where PXM was mixed with SD GLU, (Supplementary materials figure 4), showed an overlap between PXM and GLU. The phenomenon was also seen in the DSC traces of the spray-dried formulations, Figure 6a, where peaks overlapping and changes in peak intensities with respect to the drug:carrier ratio were observed.

The intense yellow colour observed in spray-dried Samples A - C has been attributed to the presence of amorphous PXM and this could be attributed to zwitterionic PXM molecules which are formed by an inter-molecular proton transfer in the amorphous form of the drug [69]. This was also confirmed by the low intensity of XRPD peaks for samples A-C. This indicates that the spray drying process in the presence of glucosamine HCl can induce some amorphous **PXM** in the samples. The XRPD **diffractograms** of PXM (Supplementary material figure 5) exhibited characteristic peaks at 8.64˚, 14.51˚, 17.70˚, 21.71 and 27.72˚ on the 2θ scale which is similar to reported peak positions observed in the cubic Form I polymorph of PXM [68]. The XRPD **diffractograms** of spray-dried PXM was similar to that observed in untreated PXM indicating no change in the PXM as a result of the spray drying process. However, since the SEM images (Supplementary materials figure 1) and DSC (Supplementary materials figure 2) of spray-dried

ACCEPTED MANUSCRIPT

PXM indicated the presence of needle shaped Form II PXM, it could be that the amount of Form II PXM recrystallized after spray drying was very small making it undetectable on the XRPD **diffractograms**. The characteristic peaks for GLU appeared at 16.73˚, 17.42˚, 27.19˚ and 31.94˚ [22]. However, after spray drying the position of these peaks changed. In addition, the peak intensities reduced significantly and this can be attributed to the process of spray drying. The significant reduction in the peak intensity of samples A-C was also attributed to the spray drying process (Figure 6b). **This phenomenon has been observed by several authors where crystalline materials have reduced peak intensities or become amorphous after the spray drying process [70, 71]**.

4. CONCLUSIONS

This study showed that spray-drying PXM alone was not sufficient to enhance the dissolution or solubility of PXM. This may be attributed to increased cohesive forces between spray dried PXM particles as compared to untreated PXM due to increased level of electrostatic charge. However, in the presence of a carrier such as **GLU**, spray drying proved to be effective at enhancing dissolution, therefore demonstrating glucosamine to be an efficient hydrophilic carrier for this process. This may be due to the relatively lack of cohesive electrostatic charge for spray dried solid dispersion particles allowing better particle wettability during dissolution. The PXM underwent some polymorphic changes during the spray drying process and this was confirmed by the SEM images and DSC traces. The dissolution rate of PXM in the solid dispersions could be optimised by varying the drug:carrier ratio to achieve the desired rate. The charge results also proved GLU to improve the handling of PXM as it significantly reduced its charge in all the spray dried formulations.

5. ACKNOWLEDGEMENTS

ACCEPTED MANUSCRIPT

The authors would like to acknowledge the University of Huddersfield for financial support and David Galiwango and Mohammed Al-nami for performing the dissolution experiments.

6. CONFLICT OF INTEREST

The authors declare no conflict of interest.

7. REFERENCES

[1] L. V. Allen Jr, Dosage form design and development, Clin.Ther. 30, (2008) 2102-2111.

[2] G. L. Amidon, H. Lennernas, V. P. Shah, and J. R. Crison, A theoretical basis for a biopharmaceutic drug classification: the correlation of in vitro drug product dissolution and in vivo bioavailability, Pharm Res, 12 (1995) 413-420.

[3] H. Al-Hamidi, A. A. Edwards, M. A. Mohammad, and A. Nokhodchi, Glucosamine HCl as a new carrier for improved dissolution behaviour: Effect of grinding, Colloids Surf., B: 81 (2010) 96-109.

[4] J. Collett and R. Moreton, Modified-release peroral dosage forms., in Aulton's Pharmaceutics: The Design and Manufacture of Medicines, ed London, UK Churchill Livingstone, (2007) 483–499.

[5] J. A. Baird and L. S. Taylor, Evaluation of amorphous solid dispersion properties using thermal analysis techniques, Adv. Drug Del. Rev. 64,(2012) 396-421.

[6] A. Fahr and X. Liu, Drug delivery strategies for poorly water-soluble drugs, Expert Opin Drug Del. 4, (2007) 403-416.

[7] K. T. Savjani, A. K. Gajjar, and J. K. Savjani, Drug Solubility: Importance and Enhancement Techniques, ISRN Pharm, 2012, (2012) 195727.

ACCEPTED MANUSCRIPT

[8] K. Asare-Addo, E. Supuk, H. Al-Hamidi, S. Owusu-Ware, A. Nokhodchi, and B. R. Conway, Triboelectrification and dissolution property enhancements of solid dispersions, Int. J Pharm, 485, (2015) 306-316

[9] B. E. Rabinow, Nanosuspensions in drug delivery, Nat Rev Drug Discov, 3, (2004) 785-796

[10] H. Valizadeh, A. Nokhodchi, N. Qarakhani, P. Zakeri-Milani, S. Azarmi, D. Hassanzadeh, and R. Lobenberg, Physicochemical Characterization of Solid Dispersions of Indomethacin with PEG 6000, Myrj 52, Lactose, Sorbitol, Dextrin, and Eudragit® E100, Drug Dev. Ind. Pharm, 30, (2004) 303-317.

[11] P. Khadka, J. Ro, H. Kim, I. Kim, J. T. Kim, H. Kim, J.M. Cho, G. Yun and J. Lee, Pharmaceutical particle technologies: An approach to improve drug solubility, dissolution and bioavailability, Asian J Pharm Sci, 9, (2014) 304-316.

[12] R. H. Müller and K. Peters, Nanosuspensions for the formulation of poorly soluble drugs: I. Preparation by a size-reduction technique, Int. J Pharm, 160, (1998) 229-237.

[13] B. B. Patel, J. K. Patel, S. Chakraborty, and D. Shukla, Revealing facts behind spray dried solid dispersion technology used for solubility enhancement, Saudi Pharm J, 23, (2015) 352-365.

[14] K. Brodka-Pfeiffer, P. Langguth, P. Grass, and H. Hausler, Influence of mechanical activation on the physical stability of salbutamol sulphate, Eur J Pharm Biopharm, 56, (2003) 393-400.

[15] J. C. Feeley, P. York, B. S. Sumby, and H. Dicks, Determination of surface properties and flow characteristics of salbutamol sulphate, before and after micronisation, Int J Pharm,172, (1998) 89-96.

[16] W. Kaialy, T. Hussain, A. Alhalaweh, and A. Nokhodchi, Towards a More Desirable Dry Powder Inhaler Formulation: Large Spray-Dried Mannitol Microspheres Outperform Small Microspheres, Pharm Res, 31, (2014) 60-76.

[17] T. Loftsson and D. Duchêne, Cyclodextrins and their pharmaceutical applications, Int J Pharm, 329, (2007) 1-11.

ACCEPTED MANUSCRIPT

[18] Y. Javadzadeh, B. Jafari-Navimipour, and A. Nokhodchi, Liquisolid technique for dissolution rate enhancement of a high dose water-insoluble drug (carbamazepine), Int J Pharm, 341, (2007) 26-34.

[19] A. Nokhodchi, Y. Javadzadeh, M. R. Siahi-Shadbad, and M. Barzegar-Jalali, The effect of type and concentration of vehicles on the dissolution rate of a poorly soluble drug (indomethacin) from liquisolid compacts, J Pharm Pharm Sci., 8, (2005) 18-25.

[20] S. E. David, P. Timmins, and B. R. Conway, Impact of the counterion on the solubility and physicochemical properties of salts of carboxylic acid drugs, Drug Dev Ind Pharm, 38 (2012) 93-103.

[21] E. Supuk, M. U. Ghori, K. Asare-Addo, P. R. Laity, P. M. Panchmatia, and B. R. Conway, The influence of salt formation on electrostatic and compression properties of flurbiprofen salts, Int J Pharm, 458 (2013) 118-127.

[22] H. Al-Hamidi, A. A. Edwards, M. A. Mohammad, and A. Nokhodchi, To enhance dissolution rate of poorly water-soluble drugs: Glucosamine hydrochloride as a potential carrier in solid dispersion formulations, Colloids Surf., B, 76, (2010) 170-178.

[23] S. Sareen, G. Mathew, and L. Joseph, Improvement in solubility of poor water-soluble drugs by solid dispersion, Int J Pharm Investig, 2, (2012) 12-17.

[24] B. Kapoor, R. Kaur, S. Kour, H. Behl, and S. Kour, Solid Dispersion: An Evolutionary Approach for Solubility Enhancement of Poorly Water Soluble Drugs, Int J Recent Adv Pharm Res, 2, (2012) 1-16.

[25] H. Takeuchi, S. Nagira, H. Yamamoto, and Y. Kawashima, Solid dispersion particles of amorphous indomethacin with fine porous silica particles by using spray-drying method, Int J Pharm, 293, (2005) 155-164.

[26] S.M. Khoo, C. J. H. Porter, and W. N. Charman, The formulation of Halofantrine as either non-solubilising PEG 6000 or solubilising lipid based solid dispersions: Physical stability and absolute bioavailability assessment, Int J Pharm, 205, (2000) 65-78.

ACCEPTED MANUSCRIPT

[27] C. R. Mashru, B. V. Sutariya, G. M. Sankalia, and P. Yagnakumar, Characterization of solid dispersions of rofecoxib using differential scanning calorimeter, J. Therm. Anal. Calorim, 82, (2005) 167-170.

[28] H. Al-Hamidi, K. Asare-Addo, S. Desai, M. Kitson, and A. Nokhodchi, The dissolution and solid-state behaviours of coground ibuprofen-glucosamine HCl , Drug Dev Ind Pharm, (2014)1-11.

[29] H. Al-Hamidi, A. A. Edwards, D. Douroumis, K. Asare-Addo, A. M. Nayebi, S. Reyhani-Rad,J. Mahmoudi and A. Nokhodchi., Effect of glucosamine HCl on dissolution and solid state behaviours of piroxicam upon milling, Colloids Surf., B, 103, (2013) 189-199.

[30] C. Leuner and J. Dressman, Improving drug solubility for oral delivery using solid dispersions, Eur J Pharm Biopharm, 50, (2000) 47-60.

[31] T. Andersson, E. Bredberg, P. O. Lagerstrom, J. Naesdal, and I. Wilson, Lack of drug-drug interaction between three different non-steroidal anti-inflammatory drugs and omeprazole, Eur J Clin Pharmacol, 54, (1998) 399-404.

[32] C. C. Da Camara and G. V. Dowless, Glucosamine sulfate for osteoarthritis, Ann Pharmacother, 32, (1998) 580-587.

[33] J. M. Pujalte, E. P. Llavore, and F. R. Ylescupidez, Double-blind clinical evaluation of oral glucosamine sulphate in the basic treatment of osteoarthrosis, Curr Med Res Opin, 7, (1980) 110-114.

[34] C. A. Tagliati, E. Kimura, M. S. Nothenberg, S. l. R. J. C. Santos, and S. Oga, Pharmacokinetic profile and adverse gastric effect of zinc-piroxicam in rats, Gen Pharmacol-Vasc S, 33, (1999) 67-71.

[35] Y. Ueno, E. Yonemochi, Y. Tozuka, S. Yamamura, T. Oguchi, and K. Yamamoto, Pharmaceutics: Characterization of Amorphous Ursodeoxycholic Acid Prepared by Spray-drying, J Pharm Pharmacol, 50, (1998) 1213-1219.

[36] O. I. Corrigan, Thermal analysis of spray dried products, Thermochim Acta, 248, (1995) 245-258.

ACCEPTED MANUSCRIPT

[37] A. Alhalaweh, A. Alzghoul, W. Kaialy, D. Mahlin, and C. A. S. Bergström, Computational Predictions of Glass-Forming Ability and Crystallization Tendency of Drug Molecules, Mol Pharm, 11, (2014) 3123-3132.

[38] D. Mahlin, S. Ponnambalam, M. Heidarian Höckerfelt, and C. A. S. Bergström, Toward In Silico Prediction of Glass-Forming Ability from Molecular Structure Alone: A Screening Tool in Early Drug Development, Mol Pharm, 8, (2011) 498-506.

[39] J. A. Baird, D. Santiago-Quinonez, C. Rinaldi, and L. S. Taylor, Role of Viscosity in Influencing the Glass-Forming Ability of Organic Molecules from the Undercooled Melt State, Pharm Res, 29, (2011) 271-284.

[40] A. Newman, G. Knipp, and G. Zografi, Assessing the performance of amorphous solid dispersions, J Pharm Sci,101(2012) 1355-1377.

[41] S. G. Maas, G. Schaldach, E. M. Littringer, A. Mescher, U. J. Griesser, D. E. Braun, P.E Walzel and N.A. Urbanetz , The impact of spray drying outlet temperature on the particle morphology of mannitol, Powder Technol, 213, (2011) 27-35.

[42] I. Duarte, M. Temtem, M. Gil, and K. Gaspar, Overcoming poor bioavailability through amorphous solid dispersions, Ind. Pharm, 30 (2011) 4-6.

[43] R. Beleca, M. Abbod, W. Balachandran, and P. R. Miller, Investigation of Electrostatic Properties of Pharmaceutical Powders Using Phase Doppler Anemometry, IEEE Trans Ind Appl, 46, (2010) 1181-1187

[44] A. G. Bailey, Charging of Solids and Powders, J Electrostat, 30, (1993) 167-180.

[45] P. C. L. Kwok and H.-K. Chan, Electrostatics of pharmaceutical inhalation aerosols, J Pharm Pharmacol, 61 (2009) 1587-1599.

[46] C. U. Yurteri, M. K. Mazumder, N. Grable, G. Ahuja, S. Trigwell, A. S. Biris, R. Sharma and R.A. Sims, Electrostatic Effects on Dispersion, Transport, and Deposition of Fine Pharmaceutical Powders: Development of an Experimental Method for Quantitative Analysis, Particul Sci Technol, 20, (2002) 59-79.

ACCEPTED MANUSCRIPT

[47] M. Faraday, XXXII. On static electrical inductive action, Philosophical Magazine Series 3, 22, (1843) 200-204.

[48] T. Hussain, W. Kaialy, T. Deng, M. S. A. Bradley, A. Nokhodchi, and D. Armour-Chélu, A novel sensing technique for measurement of magnitude and polarity of electrostatic charge distribution across individual particles, Int J Pharm, 441(2013) 781-789.

[49] A. O. Adebisi, W. Kaialy, T. Hussain, H. Al-Hamidi, A. Nokhodchi, B. R. Conway, *et al.* ., An assessment of triboelectrification effects on co-ground solid dispersions of carbamazepine, Powder Technol, 292 (2016) 342-350.

[50] P. R. Laity, K. Asare-Addo, F. Sweeney, E. Šupuk, and B. R. Conway, Using small-angle X-ray scattering to investigate the compaction behaviour of a granulated clay, Appl Clay Sci,108 (2015) 149-164.

[51] K. A. Khan, The concept of dissolution efficiency, J Pharm Pharmacol, 27 (1975) 48-49.

[52] K. Asare-Addo, W. Kaialy, M. Levina, A. Rajabi-Siahboomi, M. U. Ghori, E. Supuk, *et al.* ., The influence of agitation sequence and ionic strength on in vitro drug release from hypromellose (E4M and K4M) ER matrices--the use of the USP III apparatus, Colloids Surf B, 104(2013) 54-60.

[53] M. R. Siahi-Shadbad, K. Asare-Addo, K. Azizian, D. Hassanzadeh, and A. Nokhodchi, Release behaviour of propranolol HCl from hydrophilic matrix tablets containing psyllium powder in combination with hydrophilic polymers, AAPS PharmSciTech, 12 (2011) 1176-1182.

[54] J. W. Moore and H. H. Flanner, Mathematical comparison of dissolution profiles, Pharma Tech, 20, (1996) 64-74.

[55] J. E. Polli, L. X. Yu, J. A. Cook, G. L. Amidon, R. T. Borchardt, B. A. Burnside, et al., Summary workshop report: Biopharmaceutics classification system—implementation challenges and extension opportunities, J Pharm Sci, 93 (2004) 1375-1381.

[56] K. Asare-Addo, M. Levina, A. R. Rajabi-Siahboomi, and A. Nokhodchi, Study of dissolution hydrodynamic conditions versus drug release from hypromellose matrices: the influence of agitation sequence, Colloids Surf., B, 81 (2010) 452-460.

ACCEPTED MANUSCRIPT

[57] E. I. Nep, K. Asare-Addo, M. U. Ghori, B. R. Conway, and A. M. Smith, Starch-free grewia gum matrices: Compaction, swelling, erosion and drug release behaviour, Int J Pharm, 496 (2015) 689-698 .

[58] J. E. Polli, G. S. Rekhi, L. L. Augsburger, and V. P. Shah, Methods to compare dissolution profiles and a rationale for wide dissolution specifications for metoprolol tartrate tablets, J Pharm Sci, 86 (1997) 690-700.

[59] V. Pillay and R. Fassihi, Evaluation and comparison of dissolution data derived from different modified release dosage forms: an alternative method, J Controlled Release, 55 (1998) 45-55.

[60] D. J. Lacks and A. Levandovsky, Effect of particle size distribution on the polarity of triboelectric charging in granular insulator systems, J Electrostat, 65 (2007) 107-112 .

[61] W. Kaialy, A review of factors affecting electrostatic charging of pharmaceuticals and adhesive mixtures for inhalation, Int J Pharm, 503 (2016) 262-276.

[62] A. R. Sheth, S. Bates, F. X. Muller, and D. J. W. Grant, Polymorphism in Piroxicam, Cryst Growth Des, 4 (2004) 1091-1098.

[63] F. Vrečer, M. Vrbinc, and A. Meden, Characterization of piroxicam crystal modifications, Int J Pharm , 256 (2003) 3-15.

[64] S. Mirza, I. Miroshnyk, M. J. Habib, J. F. Brausch, and M. D. Hussain, Enhanced Dissolution and Oral Bioavailability of Piroxicam Formulations: Modulating Effect of Phospholipids, Pharmaceutics, 2, (2010) 339.

[65] F. Lai, E. Pini, G. Angioni, M. L. Manca, J. Perricci, C. Sinico and A.M. Fadda , Nanocrystals as tool to improve piroxicam dissolution rate in novel orally disintegrating tablets, Eur J Pharm Biopharm, 79 (2011) 552-558.

[66] R. Müller, C. Jacobs, and O. Kayser, DissoCubes-A novel formulation for poorly soluble and poorly bioavailable drugs, In Modified-release drug delivery systems, Rathbone MJ, Hadgraft J, and R. MS, Eds., ed New York: Marcel Dekker (2003) 135-149.

[67] M. Dixit, A. G. Kini, and P. K. Kulkarni, Preparation and characterization of microparticles of piroxicam by spray drying and spray chilling methods, Res Pharm Sci, 5 (2010) 89-97.

ACCEPTED MANUSCRIPT

[68] W. Fortunato de Carvalho Rocha, G. P. Sabin, P. H. Março, and R. J. Poppi, Quantitative analysis of piroxicam polymorphs pharmaceutical mixtures by hyperspectral imaging and chemometrics, Chemometr Intell Lab, 106 (2011) 198-204.

[69] A. R. Sheth, J. W. Lubach, E. J. Munson, F. X. Muller, and D. J. W. Grant, Mechanochromism of Piroxicam Accompanied by Intermolecular Proton Transfer Probed by Spectroscopic Methods and Solid-Phase Changes, J. Am. Chem. Soc, 127 (2005) 6641-6651.

[70] R. Pradhan, T. H. Tran, S. Y. Kim, K. B. Woo, Y. J. Choi, H. G. Choi, C.S. Yong and J. O. Kim , Preparation and characterization of fast dissolving flurbiprofen and esomeprazole solid dispersion using spray drying technique, Int J Pharm, 502 (2016) 38-46.

[71] C. Karavasili, L. Kokove, I. Kontopoulou, G. K. Eleftheriadis, N. Bouropoulos and D. G. Fatouros, Dissolution enhancement of the poorly soluble drug nifedipine by co-spray drying with microporous zeolite beta, J Drug Del Sci Technol, 35, (2016) 91-97.

ACCEPTED MANUSCRIPT

Figure captions

Figure 1. Schematic of experimental setup used in the determination of the formulations charge (a), a typical example of filtered data generated when untreated PXM particles are travelling through the sensor (b)

Figure 2. Dissolution profile of PXM, spray-dried PXM and physical mixtures with different ratios of drug:carrier (a), dissolution profile of PXM, physical mixtures of PXM with spray-dried glucosamine (b) **(SD, n=3)**

Figure 3. SEM images of spray dried solid dispersions of PXM: GLU in a 1:1 ratio (Sample A) (a), PXM: GLU in a 1:2 ratio (Sample B) (b)

Figure 4. Positive charge-to-mass ratio (P-CMR), negative charge-to-mass ratio (N-CMR) and net charge-to-mass ratio (Net-CMR) for untreated PXM, spray dried PXM (a); untreated GLU and spray dried GLU (b) **(SD, n=3)**

Figure 5. Positive charge-to-mass ratio (P-CMR), negative charge-to-mass ratio (N-CMR) and net charge-to-mass ratio (Net-CMR) for untreated PXM, untreated GLU and spray-dried solid dispersions (a) dissolution profiles of PXM and spray-dried solid dispersions (b) **(SD, n=3)**

Figure 6. DSC thermograms of spray-dried solid dispersions of PXM: GLU in a 1:1 ratio (Sample A), PXM: GLU in a 1:2 ratio (Sample B) and PXM: GLU in a 2:1 ratio (Sample C) (a), XRPD patterns of spray-dried dispersions of PXM: GLU in a 1:1 ratio (Sample A), PXM: GLU in a 1:2 ratio (Sample B) and PXM: GLU in a 2:1 ratio (Sample C) (b)

ACCEPTED MANUSCRIPT

Tables

Table 1. Effects of spray drying and carrier type on dissolution parameters of PXM **(SD, n=3)**

Piroxicam (PXM):carrier	Carrier	DE_{120min} (%)	$MDT_{(min)}$	$MDR_{(\%min^{-1})}$	Q_{10min} (%)	Q_{20min} (%)	Q_{30min} (%)
Untreated PXM	-	21.2±0.5	7.8±0.6	0.18±0.02	8.5±0.4	11.9±0.2	17.5±1.8
SD PXM	-	20.6±5.8	7.7±0.8	0.2±0.08	10.3±1.2	15.4±2.5	19.0±4.9
PM1:1		21.6±5.2	3.6±0.3	0.12±0.06	8.1±1.4	10.7±2.2	13.4±3.1
PM1:2		21.2±0.5	6.98±0.2	0.17±0.01	8.5±1.0	12.3±0.5	17.4±0.8
PM2:1		19.1±3.4	4.22±0.1	0.13±0.03	7.6±0.4	10.3±1.8	12.8±1.7
1:1 SD GLU	SD GLU	33.2±9.4	7.5±1.4	0.33±0.1	9.9±0.7	21.1±4.7	27.5±8.1
1:2 SD GLU	SD GLU	38.0±10.3	6.8±1.5	0.37±0.1	13.1±2.4	22.4±8.5	29.6±11.1
2:1 SD GLU	SD GLU	16.4±2.0	4.8±0.4	0.12±0.01	7.4±0.04	10.1±0.2	12.4±0.5
Sample A (1:1)		38.9±3.8	5.6±1.7	0.38±0.10	26.3±3.2	31.7±5.7	37.8±6.8
Sample B (1:2)		31.1±3.4	3.7±0.7	0.25±0.05	15.3±1.3	19.9±2.5	22.2±3.4
Sample C (2:1)		56.7±4.7	6.0±2.6	0.53±0.13	25.4±3.6	32.0±2.9	43.6±7.2

ACCEPTED MANUSCRIPT

Table 2. Solubility of PXM in the formulations. PXM in the presence of a carrier at different concentrations and PXM before and after spray drying **(SD, n=3)**.

Samples	Amount of drug in solution (mg/L)
Sample A (1:1)	32.6 ± 1.8
Sample B (1:2)	15.5 ± 1.6
Sample C (2:1)	19.5 ± 1.3
Untreated PXM	20.7 ± 0.9
Spray-dried PXM	17.7 ± 1.2
1% GLU	17.4 ± 0.6
5% GLU	20.1 ± 0.5
10% GLU	22.8 ± 0.7
15% GLU	23.4 ± 0.5

Figures

ACCEPTED MANUSCRIPT

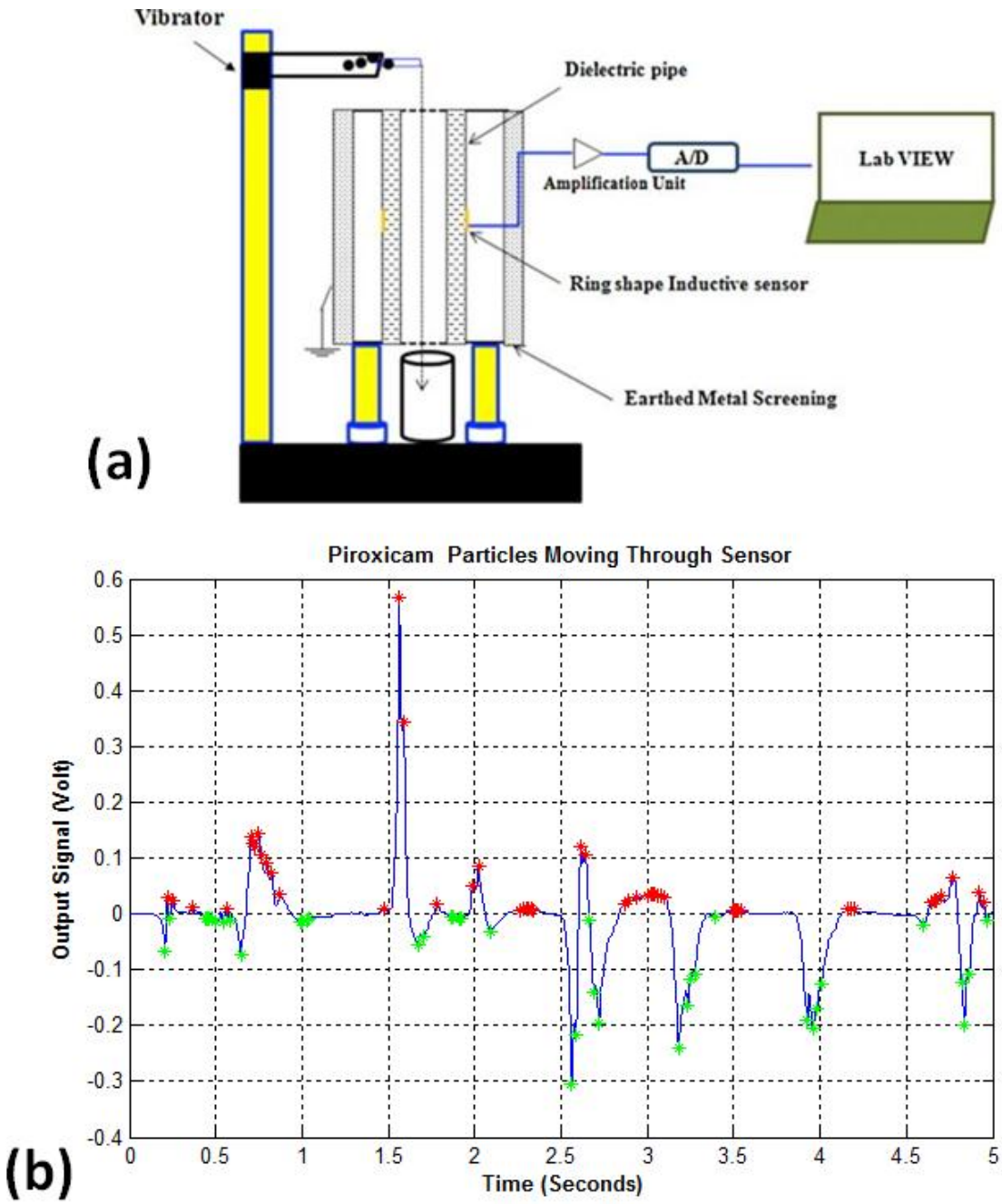

Figure 1

ACCEPTED MANUSCRIPT

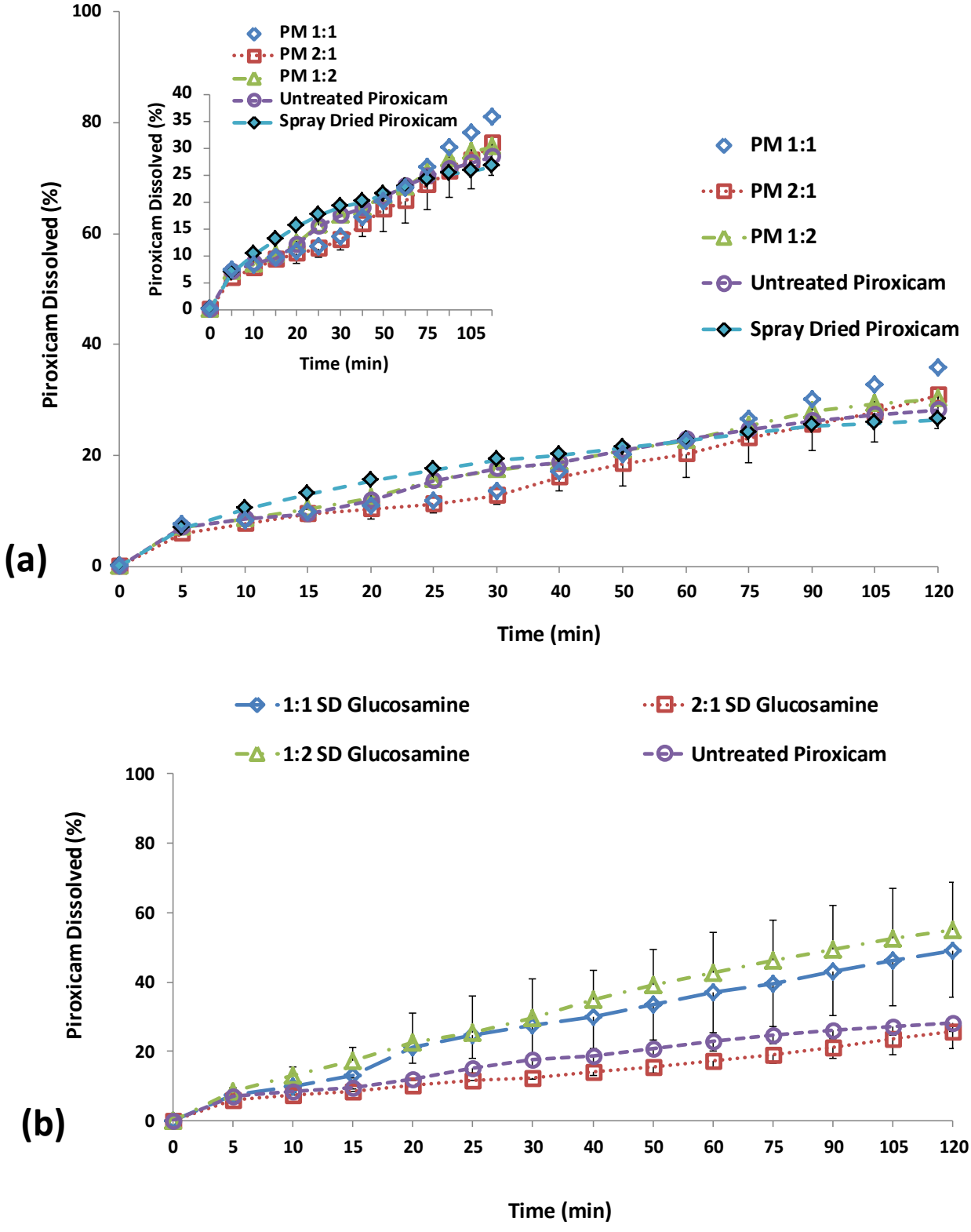

Figure 2

ACCEPTED MANUSCRIPT

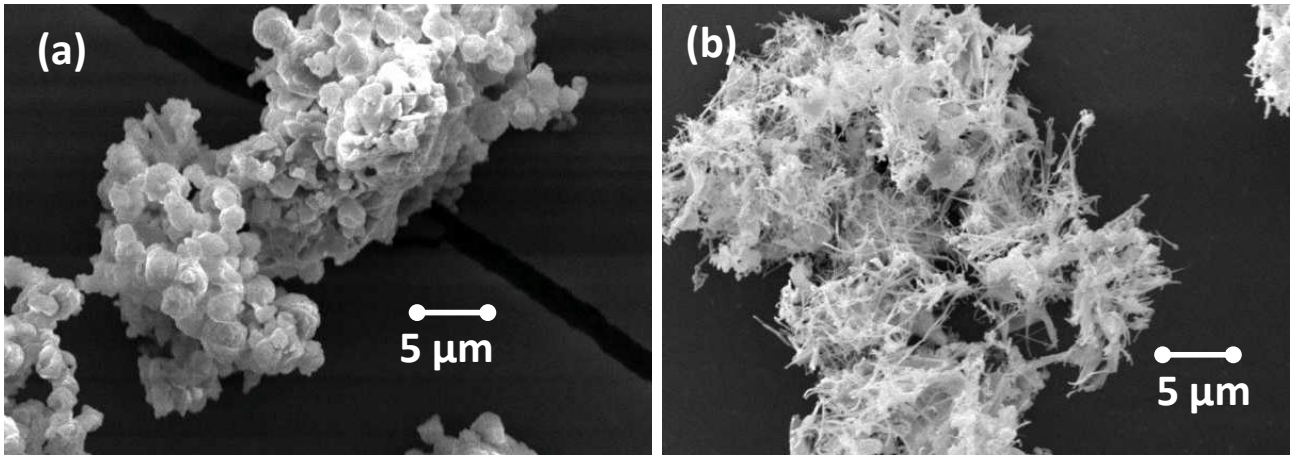

Figure 3

ACCEPTED MANUSCRIPT

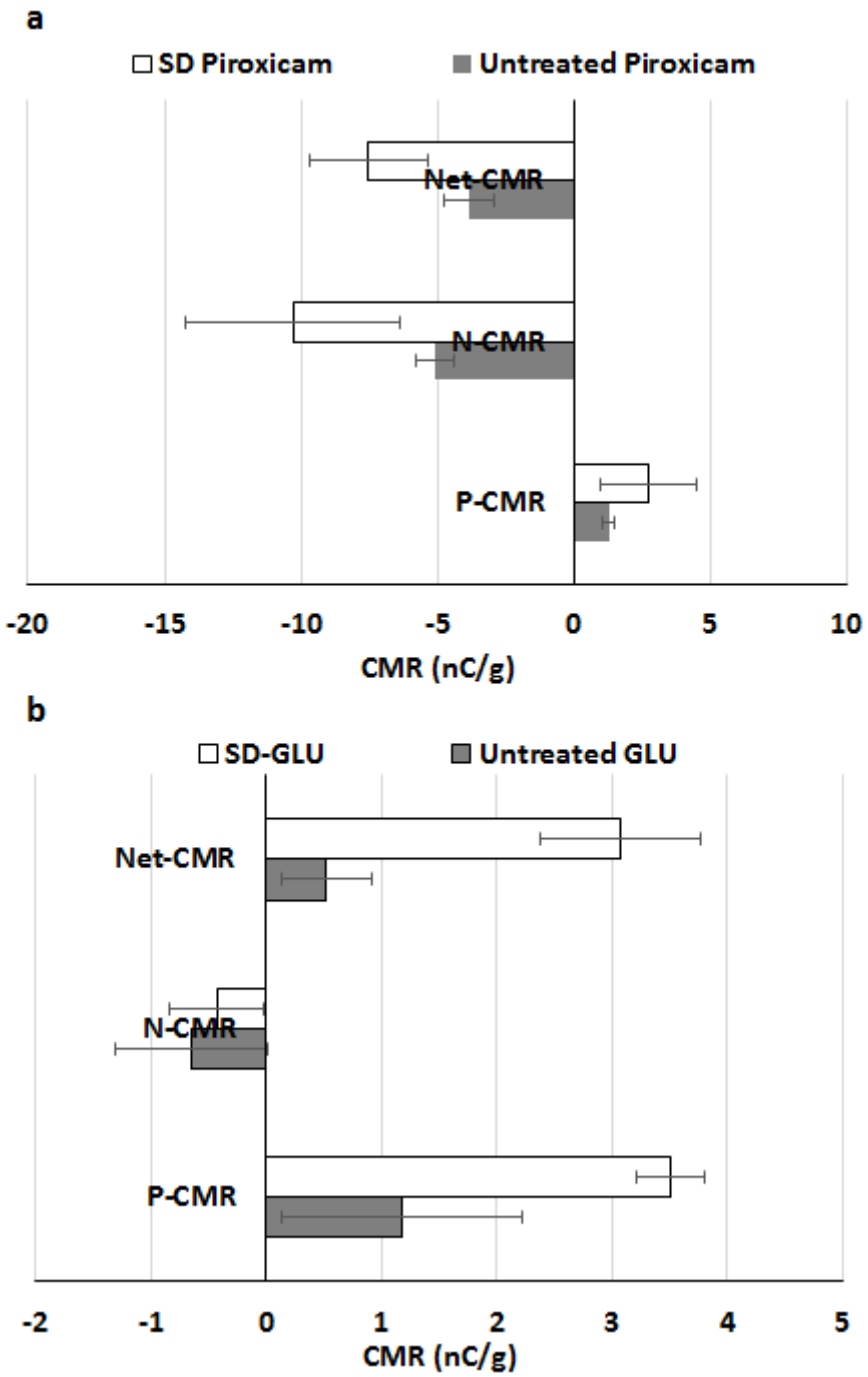

Figure 4

ACCEPTED MANUSCRIPT

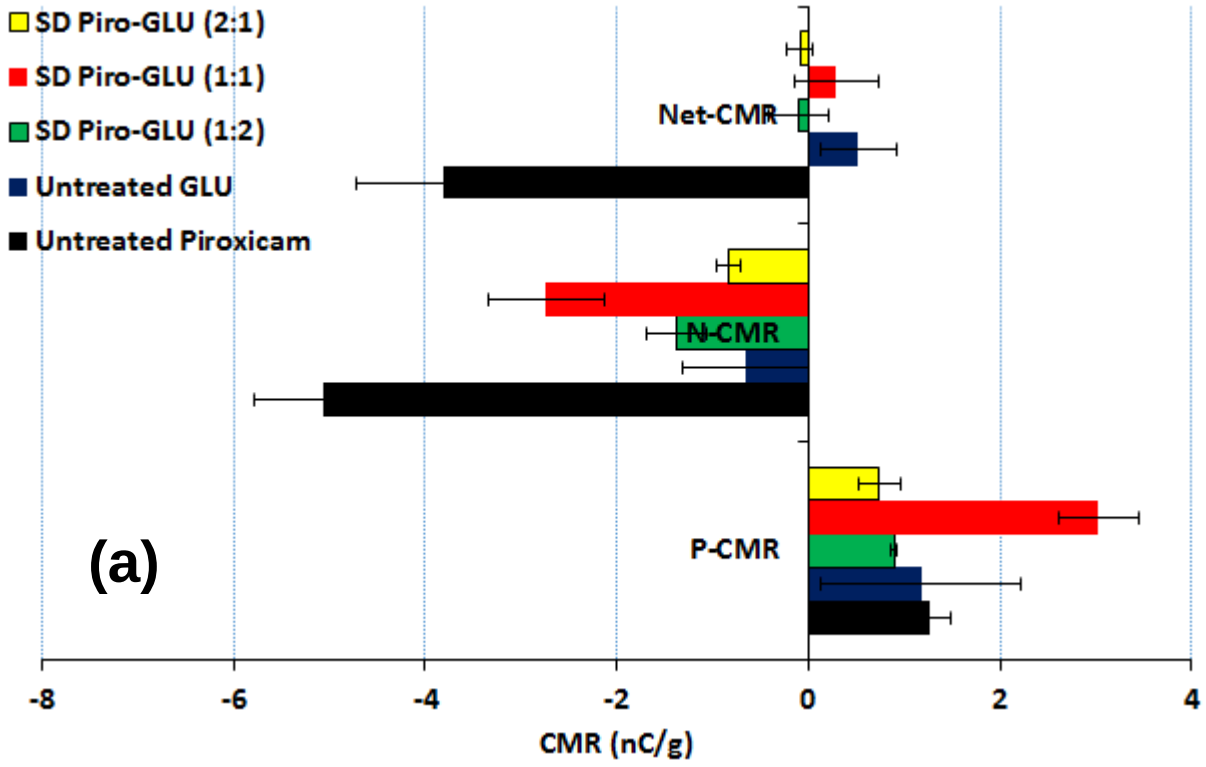

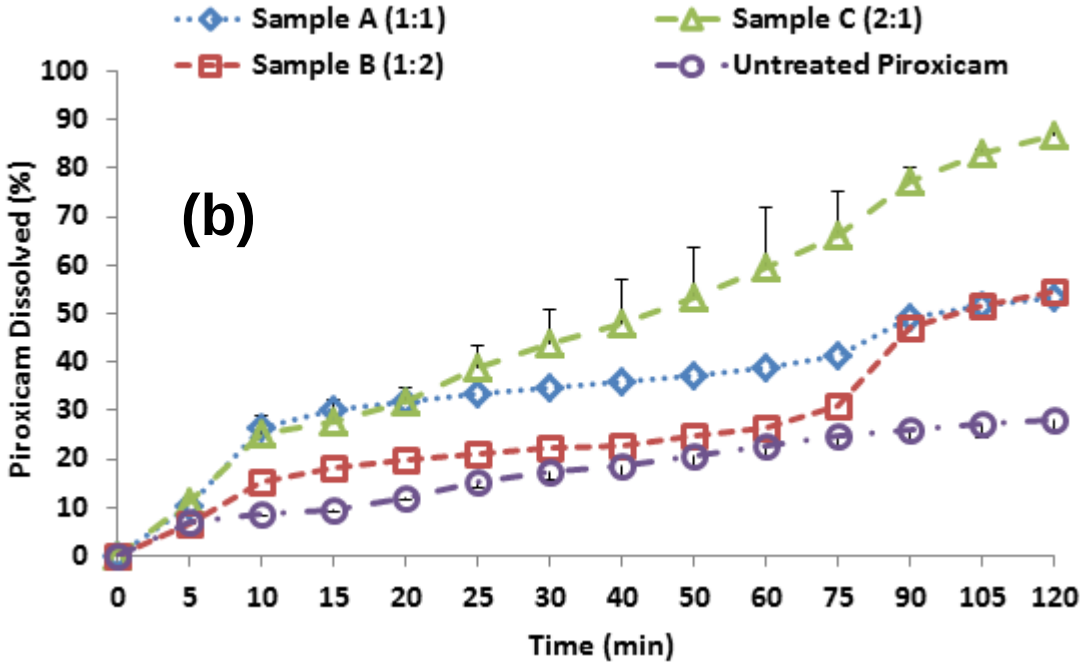

Figure 5

ACCEPTED MANUSCRIPT

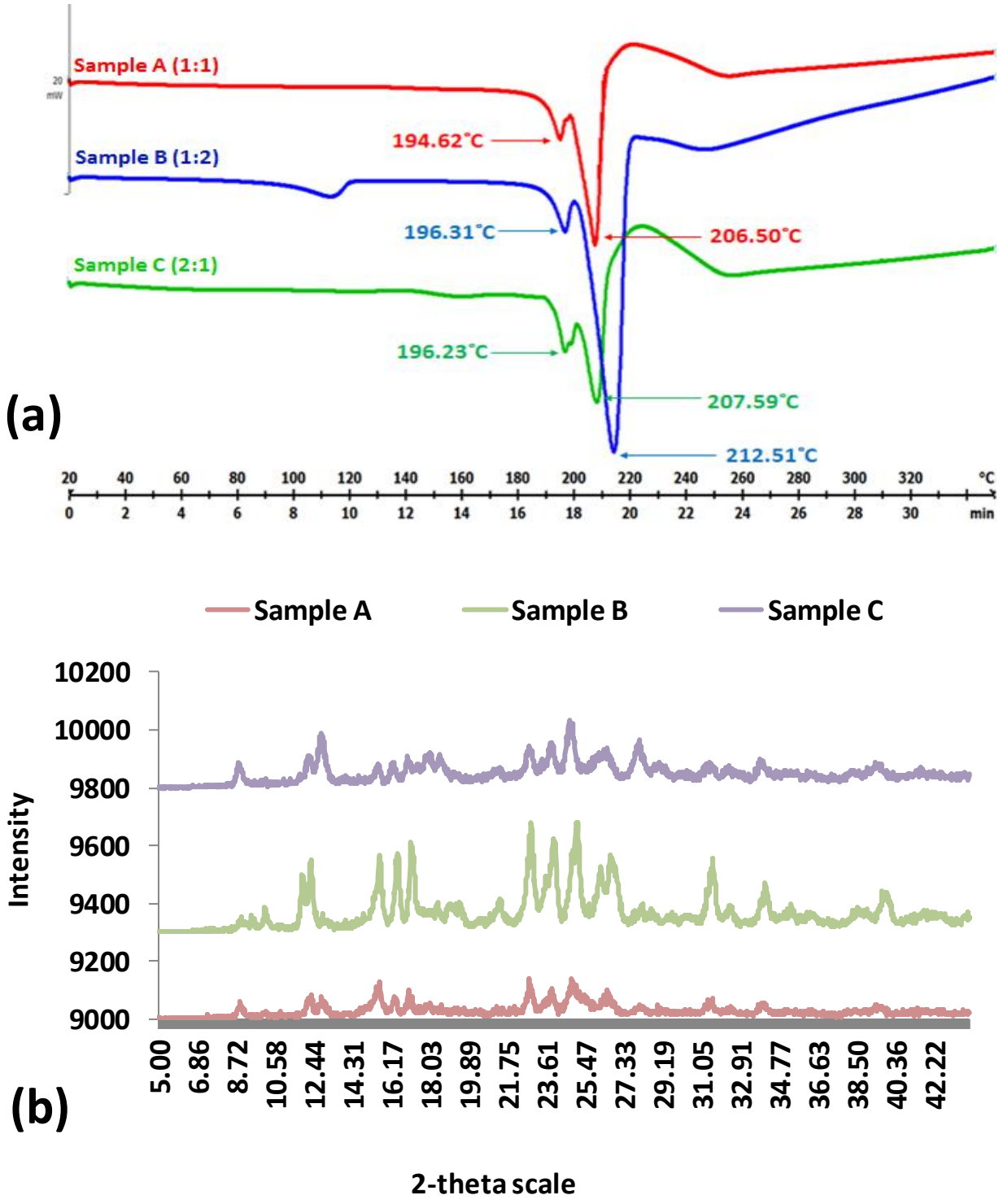

Figure 6

ACCEPTED MANUSCRIPT

Graphical abstract

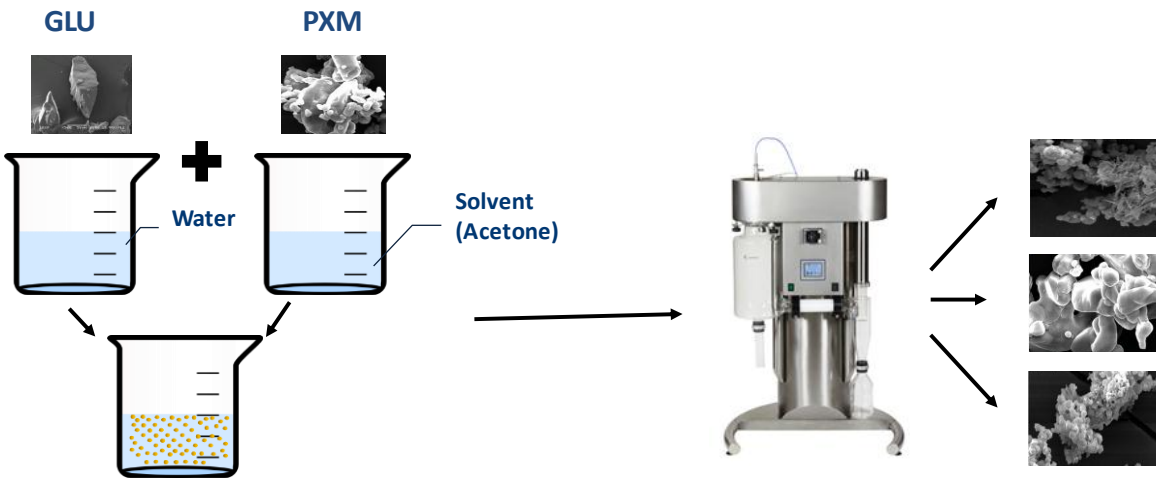

Piroxicam (PXM) and glucosamine (GLU) spray dried solid dispersions